MRS Advances © 2019 Materials Research Society
DOI: 10.1557/adv.2019.259

Synthesis and Characterization of 2D-Graphene Oxide-Metal Hybrid Systems with Increased Solubility

Hadi Kelani[1], Shelby Weatherbee[1], Stephen Blama[1] and Mary Sajini Devadas[1]*

[1]*Department of Chemistry, Towson University 8000 York Road, Towson, MD 21252, U.S.A.*

**Corresponding Author Email: mdevadas@towson.edu*

ABSTRACT

Graphene oxide serves as a precursor to various technologies, which include batteries, biosensors, solar cells, and supercapacitors. Gold nanoparticles exhibit excellent electrochemical and photophysical properties, allowing for electronic absorption and the ability to absorb light energy at the plasmonic wavelength. Palladium nanoparticles are highly sensitive and functional in room temperature, making it an ideal metal for catalytic applications. We report the synthesis of functional graphene oxide from graphite flakes followed by the insertion of gold and palladium nanoparticles through an oleylamine ligand. In this report, the fermi level of graphene oxide (GOx), gold-graphene oxide (Au-GOx), and palladium-graphene oxide (Pd-GOx) was shown to be effectively controlled. Additionally, each system showed complete solubility in ethanol and in the case of Au-GOx, enhanced solubility was seen in tetrahydrofuran as well.

INTRODUCTION

Graphene oxide (GOx) serves as a precursor to applications such as batteries, biosensors, solar cells, and support systems for metal catalysts [1]. Graphene oxide consists of an increased number of oxygen-containing functional groups, ultimately functionalizing the system. The carboxyl groups aid in solvent solubility, preserve graphene properties, and prevent agglomeration [2]. In this experiment, GOx was synthesized to support a metal-complex. The primary metals used in this paper were gold and palladium.

Gold nanoparticles exhibit excellent electrochemical and photophysical properties, allowing for electronic absorption and the ability to absorb light energy at the plasmonic wavelength [3]. Gold nanoparticles inserted on the surface of GOx generate a localized surface plasmon resonance, which is the result of the oscillation of conduction band electrons in the gold nanoparticles excited by light [4]. Applications for Au-GOx hybrid systems include nerve agent sensing, catalysis, biomedical probes for various diseases, and removal of cancer cells [5-7].

Palladium nanoparticles are highly selective, sensitive, and functional in room temperature [8, 9]. Palladium is also resistant to oxidation and consists of a high surface area to volume ratio, making it an ideal metal for catalytic applications [10]. These characteristics allow the nanoparticle to be a cheap and stable alternative transition metal in the catalysis of Suzuki cross coupling reactions. A Suzuki cross coupling reaction is a palladium-catalyzed coupling reaction between an organohalide and a boronic acid, introducing a newly formed carbon-carbon bond. Palladium nanoparticles also intensify the interaction between the surface of the complex and the hydrogen molecules, enabling for hydrogen gas sensing analysis [9]. The fermi levels for both graphene-oxide and metal graphene-oxide hybrids was effectively controlled. The fermi level represents an energy barrier for electrons and stimulates performance rate in systems [11]. Both graphene-oxide and metal-graphene oxide were also found to be completely soluble in ethanol despite the oxygen containing functional groups.

EXPERIMENTAL DETAILS

Synthesis of Graphene Oxide

Graphite powder was oxidized using a variation of the Tour method [12]. Graphite powder was mixed with potassium permanganate, followed by the addition of a 9:1 mixture of sulfuric acid and phosphoric acid. The reaction was refluxed at 50℃ for approximately three days. The refluxing duration determines its oxidation stage. The mixture was then cooled to room temperature, followed by the addition of hydrogen peroxide and ice cold milli-Q water. The reaction was then washed through centrifugation using water, 30% HCl, and ethanol (3x).

Synthesis of Au-GOx

12.8 mg of graphene oxide was dispersed in 100 mL tetrahydrofuran (THF) followed by ultrasonication until an even suspension of GOx was reached. 1.520 mmol oleylamine was added to the solution followed by 5.91 mg of gold(III) chloride trihydrate, and the reaction was left stirring for 24 hours under room temperature. 2.37 mg of sodium borohydride was then added to the mixture, and the product was rotary evaporated to obtain a dried Au-GOx product. The oleylamine ligand successfully dissolved the product in THF following rotary evaporation.

Synthesis of Pd-GOx

12.8 mg of graphene oxide was dispersed in ethanol followed by ultrasonication until an even suspension of GOx was reached. 300 µL oleylamine was added to the solution and mixed for thirty-minutes. 5.8 mg of palladium acetate was then added to the mixture and the reaction was left stirring for 36 hours under room temperature. 2.2 mg of sodium borohydride was then added to the mixture after dissolving the solid in the least

amount of solvent. The product was then washed through centrifugation using ethanol (3x).

UV-Vis spectroscopy

A Varian Cary UV-Vis spectrophotometer was utilized to characterize the samples to look for the obvious optical signatures to prove the transformation of the samples. Each sample was prepared in a quartz cuvette. Ethanol was utilized as the blank, as every sample was soluble in the solvent. Samples were generally diluted to an optical density of 0.1 and data was subsequently normalized. All samples analysed were in solution to minimize scattering effects of any suspended material.

Fluorescence spectroscopy

Steady state fluorescence was used to measure fluorescence and quantum yield of the samples. All samples were excited at 300 nm. Fluorescence measurements were conducted using a Jobin-Yvon Fluoromax 4 fluorescence spectrophotometer. All samples were analyzed immediately following UV-Vis determinations and were in the same quartz cuvettes with the same optical density unless otherwise noted. Slit widths in each case were set at 3 and 5 nm for the excitation and emission slits respectively. The standard was p-terphenyl.

Infrared spectroscopy

IR measurements were conducted using a Nicolet Fourier Transform - Infrared (FT-IR-ATR) spectrometer. All samples were tested as dried products and analyzed using the solid FT-IR capabilities. The technique was utilized to determine the functional groups in our samples.

Transmission electron microscopy (TEM) and Scanning electron microscopy (SEM)

TEM analysis was done at FEI Corporation. Samples were imaged on a Talos F200X 200kV instrument. Samples were suspended in ethanol, drop-casted on holey carbon grids, and were imaged after drying. SEM imaging was done on a LoVac Apreo 30 kV instrument. Samples were drop-casted on silicon wafers and air dried before imaging.

Raman spectroscopy data collection

A Rigaku Progeny X2 Handheld Raman Analyzer was utilized to measure the vibrational state of our samples. A 785 nm laser was utilized to illuminate the sample. Each sample was dissolved in ethanol and placed in a 4 mL glass vial to record the spectra.

DISCUSSION

In this study we synthesized and characterized gold nanoparticles supported on graphene oxide (Au-GOx), graphene oxide (GOx), and palladium nanoparticles on graphene oxide (Pd-GOx), using modified literature procedures [6, 12]. UV-Vis spectroscopy, fluorescence spectroscopy, infrared spectroscopy, transmission electron

microscopy, Raman spectroscopy, and carboxylic acid estimation through the generation of a calibration curve using methylene blue was used to characterize the samples. Figure 1A describes the optical signature of the three products named above. In Figure 1A, the notable peak at ~250 - 300 nm is characteristic of GOx. In regards to the Au-GOx, the GOx peak disappears and a newly formed peak at ~300 nm forms. In the case of Pd-GOx, a peak at ~280 nm is formed. The newly formed peaks for both metal-complexes are due to interactions between the metal and the graphene-oxide surface. The peaks identified for GOx correspond to the expected $\pi \rightarrow \pi^*$ and $n \rightarrow \pi^*$ electron transitions [13]. In the Au-GOx product, we see the creation of a surface plasmon peak at 530 nm. The broad nature of the surface plasmon peak indicates an unequal size distribution of gold particles on the surface [14]. A similar shoulder is observed for the Pd-GOx sample. The slight difference in the peaks associated with these electronic transitions can be attributed to the percent loading of the metal nanoparticles as well as the amount of oxygen centers created on the surface of GOx.

Figure 1B is the steady fluorescence spectra measured at an excitation wavelength of 300 nm. Quantum yield measurements were made in order to estimate the fluorescence of the material for sensing applications. The fluorescent dye used as standard for these experiments, p-terphenyl has a known quantum yield of 0.93 [15]. The quantum yield is shown in Table 1. Pd-GOx had the highest quantum yield (Φ) with 3×10^{-1} followed by GOx with a Φ of 6.09×10^{-2} and the lowest was Au-GOx at 2.34×10^{-3}. This was expected because of a higher percent loading of Au when compared to Pd on GOx.

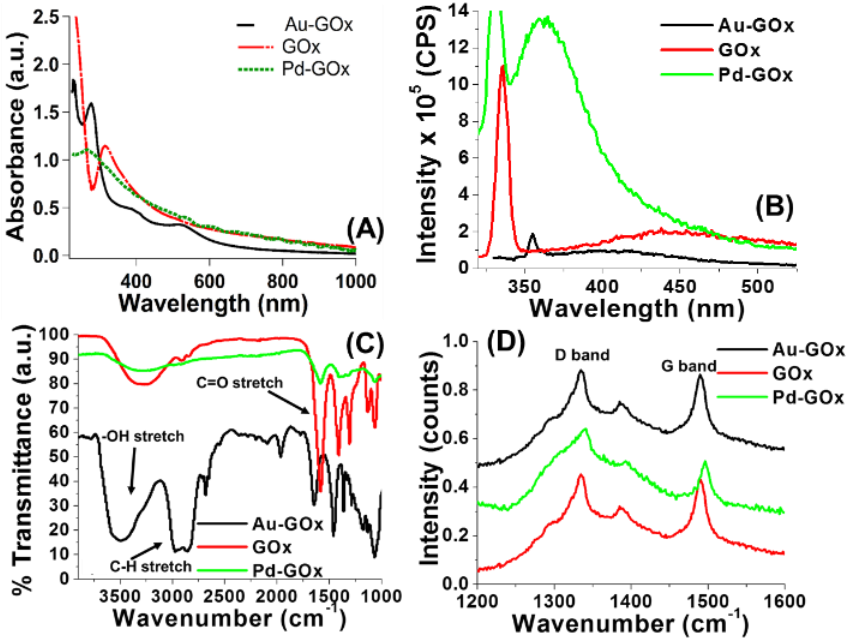

Figure 1. Characterization of the products (A) UV-Vis spectra comparing Au-GOx, GOx, and Pd-GOx (B) Steady State Fluorescence spectra comparing Au-GOx, GOx, and Pd-GOx utilizing 300 nm as excitation wavelength (C) IR spectra comparing Au-GOx, GOx, and Pd-GOx, showing functional groups characteristic of carboxylic acid groups (D) Raman spectra comparing Au-GOx, GOx, and Pd-GOx, exhibiting D and G bands found in all three systems.

Table 1. Quantum Yield Data

Sample Name	Solvent	Excitation Wavelength (nm)	Quantum Yield
Au-GOx	Ethanol	300	2.34×10^{-3}
GOx	Ethanol	300	6.09×10^{-2}
Pd-GOx	Ethanol	300	3.0×10^{-1}

Figure 1C compares the infrared spectra of the three systems. The most notable peaks of the samples are the –OH stretch at ~3200-3500 cm^{-1} and the C=O stretch at ~1600 cm^{-1}. The existence of these peaks confirms the presence of carboxyl (O = C–OH) groups created on the graphite sheets [16].

Figure 1D indicates the characteristic D and G bands found in GOx and GOx-metal hybrid systems through the generation of a Raman spectrum. The D band is assigned as the defect band, which is the result of the disordered structure of graphene. The G band is attributed to the formation of graphene oxide; indicating the presence of sp^2 carbons [17]. Raman spectra show D peaks ~1500 cm^{-1} and G peaks ~1350 cm^{-1}, confirming the lattice distortions. The sp^2 network created should allow for storage of charge and delocalization. Even though oxidized, the GOx sheets will retain sufficient periodicity in the conjugated network owing to the surfacing with metals such as Au and Pd.

Figure 2A represents the TEM image of Au-GOx, showing the presence of gold nanoparticles surfaced on the graphene oxide sheets. Figure 2B strictly shows the graphene oxide sheets unbound to any type of metals. Figure 2C shows the SEM image of the palladium nanoparticles (bright spots) laid on the surface of the sheets.

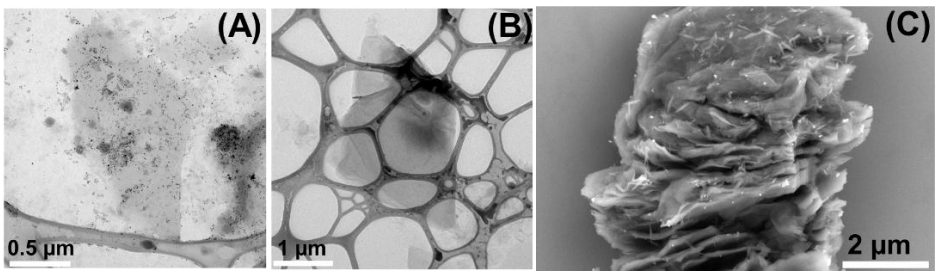

Figure 2. Electron Microscopy analysis. (A) TEM image of Au-GOx (B) TEM image of GOx (C) SEM image of Pd-GOx

Fermi level

In order to analyze the amount of carboxylic acid groups within the graphene oxide, the process of methylene blue bleaching was performed [18]. Methylene blue reacts in a 1:1 ratio with carboxylic acid; therefore, each reacting methylene blue molecule is equivalent to a reacting carboxylic acid group. The concentration of carboxylic acids was determined experimentally through UV-Vis and through the generation of a calibration curve. The deviation between the concentrations of GOx compared with GOx samples reacting with methylene blue was proportional to the reacting carboxylic acid content. The carboxylic acid molecules within the GOx samples are quantifiable. The fermi level for the collected samples was then calculated from the Nernst equation and the standard hydrogen electrode reduction potential of the methylene

blue to reduced-methylene blue reaction. The initial reaction quotient ln(Q) was calculated before and after the reaction with methylene blue to determine the reduction potential for the GOx samples. In the calculation below they are 5.0982 x 10^{15} and 1.8074 x 10^{18} respectively.

Fermi Level Sample Calculation

Applying Nernst equation:

$$E_{GO|RGO} = E_{MB|RMB} - \frac{RT}{nF}\ln(Q)$$

$$E_{GO|RGO} = 0.01\,V - \frac{(8.314\,Jmol^{-1}K^{-1})\,(298\,K)}{(1\,e^{-})(95484.56\,Cmol^{-1})}\ln\left(\frac{5.0982\,x\,10^{15}}{1.8074\,x\,10^{18}}\right)$$

$$E_{GO|RGO} = 0.162329$$

$$E_{GO|RGO} = 162.33\,mV$$

Figure 3A is the methylene blue calibration curve generated to compare the carboxylic acid content and fermi level values of GOx and Au-GOx. The fermi level represents the chemical potential for the electrons, and is the energy level of the electron at absolute zero temperature [17]. As shown in Table 2, GOx was shown to have a higher fermi level, and the data for Au-GOx was below the limit of quantification. Figure 3B is a second methylene blue calibration curve used to compare the carboxylic acid content and fermi level values between GOx and Pd-GOx. Table 2 shows Pd-GOx to have a higher fermi level at 185 mV than GOx which was at 162.33 mV due to lower carboxylic acid content. Au-GOx had the lowest value below the limit of quantification due to higher percent loading of Au.

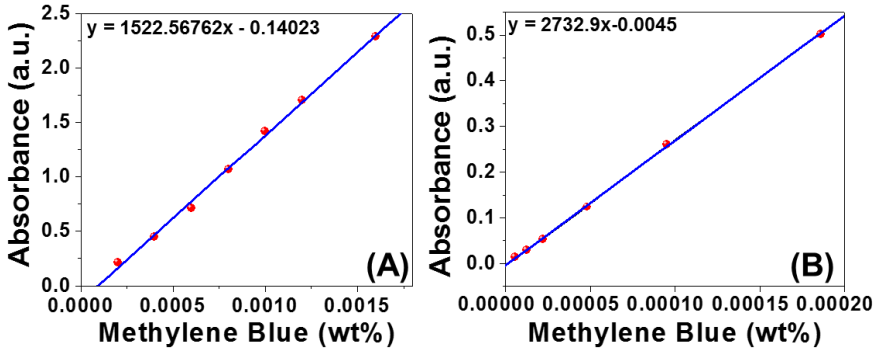

Figure 3. (A) Methylene blue calibration curve used for synthesis of Au-GOx (B) Methylene blue calibration curve used for synthesis of Pd-GOx

Table 2. Fermi Level Data

Sample	Blank Corrected Absorbance at 664 nm	MB Concentration (wt%)	COOH per mg (mol)	Fermi Level (mV)
GOx (used for Au-GOx synthesis)	0.4128	0.0003632	2.33×10^{19}	11.80
Au-GOx	2.5090	0.001740	Below LOQ	Below LOQ
GOx (used for Pd-GOx synthesis)	0.357	0.000132	5.10×10^{15}	162.33
Pd-GOx	0.452	0.000167	1.79×10^{15}	189.45

Solubility studies

Most literature work focusses on reduced graphene oxide and not graphene oxide [1, 12]. Pd-GOx has been synthesized utilizing the Tour method but without the reduction of graphene-oxide. In addition, the oxidation period was increased to 72 hours from 12 hours to form increased oxygen sites. Therefore, by not reducing our samples, we have been able to dissolve our Pd-GOx in organic solvents such as ethanol and acetone, and water. We performed a time-dependent study for Pd-GOx and Au-GOx dissolved in ethanol (10% solution). Figure 4 shows that the samples were stable for about 72 hours. Additionally, Au-GOx was also soluble in tetrahydrofuran for more than 3 days.

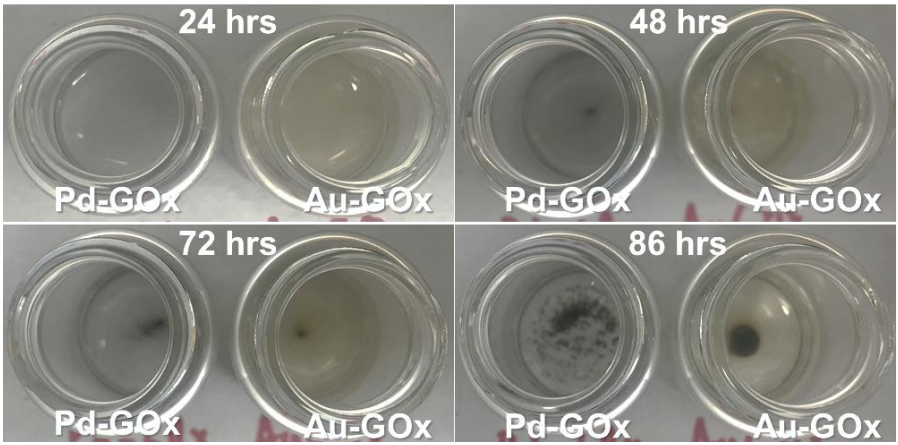

Figure 4. Solubility of Pd-GOx and Au-GOx in ethanol over the course of 86 hours

CONCLUSION

Graphene oxide was synthesized followed by the surfacing of gold and palladium nanoparticles. Each system, Pd-GOx and Au-GOx was completely soluble in ethanol, and Au-GOx was also exceptionally soluble in tetrahydrofuran allowing for the collection of data using various characterization techniques. For Au-GOx, GOx, and Pd-GOx, the following characterization techniques were utilized: UV-Vis spectroscopy, fluorescence, infrared spectroscopy, transmission electron microscopy, Raman spectroscopy, and carboxylic acid estimation through the generation of a methylene blue calibration curve. The fermi level of each system was controlled, as each sample

possessed a characteristic value representative of the highest energy state occupied by the electrons at absolute zero temperature. This shows that controlling the loading of the metal nanoparticles on the GOx surface controls the fermi level and thereby can lead to tailor made electronic materials.

ACKNOWLEDGMENTS

This research was funded by Towson University's Fisher College of Science and Mathematics Endowment Grant, Fisher Endowed Chair Grant, Undergraduate Research Grant, Raspet Summer Research fellowship, Faculty Development and Research Committee Grant, Graduate student association research grant. We also acknowledge support from NSF MRI NO.1626326. We also thank FEI Corporation for help with TEM analysis.

REFERENCES

[1] I.V. Lightcap, T.H. Kosel, P.V. Kamat, Nano Letters, **10,** 577-583 (2010).
[2] V.V. Neklyudov, N.R. Khafizov, I.A. Sedov, A.M. Dimiev, Physical Chemistry Chemical Physics, **19,** 17000-17008 (2017).
[3] X. Huang, M.A. El-Sayed, Journal of Advanced Research, **1,** 13-28 (2010).
[4] S. Eustis, M.A. El-Sayed, Chemical Society Reviews, **35,** 209-217 (2006).
[5] L. Shao, X. Huang, D. Teschner, W. Zhang, ACS Catalysis, **4,** 2369-2373 (2014).
[6] R.V. Olkhov, A.M. Shaw, RSC Advances, **4,** 31678-31684 (2014).
[7] K. Turcheniuk, R. Boukherroub, S. Szunerits, Journal of Materials Chemistry B, **3** (2015) 4301-4324.
[8] X. Chen, G. Wu, J. Chen, X. Chen, Z. Xie, X. Wang, Journal of the American Chemical Society, **133,** 3693-3695 (2011).
[9] A. Sanger, P.K. Jain, Y.K. Mishra, R. Chandra, Sensors and Actuators B: Chemical, **242,** 694-699 (2017).
[10] R.S. Erami, D. Díaz-García, S. Prashar, A. Rodríguez-Diéguez, M. Fajardo, M. Amirnasr, S. Gómez-Ruiz, Catalysts, **7,** 76 (2017).
[11] Y. Liu, P. Stradins, S.- H. Wei, Science Advances, **2,** e1600069 (2016).
[12] D.C. Marcano, D.V. Kosynkin, J.M. Berlin, A. Sinitskii, Z. Sun, A. Slesarev, L.B. Alemany, W. Lu, J.M. Tour, ACS Nano, **4,** 4806-4814 (2010).
[13] N.G. Hussain, A.; Sarma, R. K.; Sharma, P.; Barras, A.; Boukherroub, R.; Saikia, R.; Sengupta, P.; Das, M.R., ChemPlusChem, **79,** 1774-1784 (2014).
[14] M.S. Devadas, K. Kwak, J.-W. Park, J.-H. Choi, C.-H. Jun, E. Sinn, G. Ramakrishna, D. Lee, The Journal of Physical Chemistry Letters, **1,** 1497-1503 (2010).
[15] R.S. Katoh, K.; Furube, A.; Kotani, M.; Tokumaru, K., J. Phys. Chem. C, 113 (2009) 2961-2965.
[16] J.G. Radich, P.V. Kamat, ACS Nano, **7,** 5546-5557 (2013).
[17] P. Lian, X. Zhu, S. Liang, Z. Li, W. Yang, H. Wang, Electrochimica Acta, **55,** 3909-3914 (2010).
[18] K.C. Nguyen, Advances in Natural Sciences: Nanoscience and Nanotechnology, **3,** 045008 (2012).